PCCP

Molecular simulations of adsorption and siting of light alkanes in silicalite-1

R. Krishna* and D. Paschek

Department of Chemical Engineering, University of Amsterdam, Nieuwe Achtergracht 166, 1018 WV Amsterdam, The Netherlands. E-mail: krishna@its.chem.uva.nl

Received 3rd October 2000, Accepted 7th December 2000
First published as an Advance Article on the web 9th January 2001

Configurational-bias Monte Carlo (CBMC) simulations have been used to determine the sorption isotherms of methane, ethane, propane, n- and isobutane in silicalite-1 at 300 K. The equilibrium molecular loadings were determined separately for the straight and zig-zag channels and at the channel intersections. The sorption strengths for each of these locations are different, in general. In particular, isobutane molecules have a strong preference for locating at the channel intersections. The pure component isotherms, obtained from CBMC simulations, could be fitted with a 3-site Langmuir model and are in good agreement with experimental data from the literature. CBMC simulations were also used to determine the sorption isotherms for mixtures of methane–propane, methane–n-butane, n-butane–isobutane and propane–isobutane. The mixture isotherms could be predicted from the pure component isotherms using the ideal adsorbed solution theory (IAST), taking into account the detailed information on the sitings of molecules within the silicalite-1 matrix.

1 Introduction

Zeolites are widely used in the chemical industries as adsorbents and catalysts.[1–3] Of the many existing zeolitic structures, silicalite-1 is perhaps the most studied, best characterised and the most widely used in practice. Silicalite-1 provides a non-polar structure for adsorption of relatively small molecules and recently there has been an upsurge of activity in the use of silicalite-1 membranes for separation of mixtures of light hydrocarbons.[4–11] Silicalite-1 has a high ratio of silica to alumina, is hydrophobic and stable up to high temperatures. Fig. 1 shows a schematic of the structure of silicalite-1 which consists of a system of intersecting channels composed of zig-zag channels along x, cross-linked by straight channels along y. Both channels are defined by 10-rings. The straight channels are approximately elliptical in shape having a 0.53 nm × 0.56 nm cross section while the zig-zag channels have a 0.51 nm × 0.55 nm cross section, see Fig. 1.

For the development of silicalite membrane processes to separate mixtures of light hydrocarbons, information is required on both the diffusion and sorption of pure components, and their mixtures. Both experimental[12–19] and theoretical studies[20–33] on the sorption and diffusion of light hydrocarbons in silicalite have been reported in the literature.

For description of the pure component isotherms, the 2-site Langmuir (2SL) model has been used by several workers to

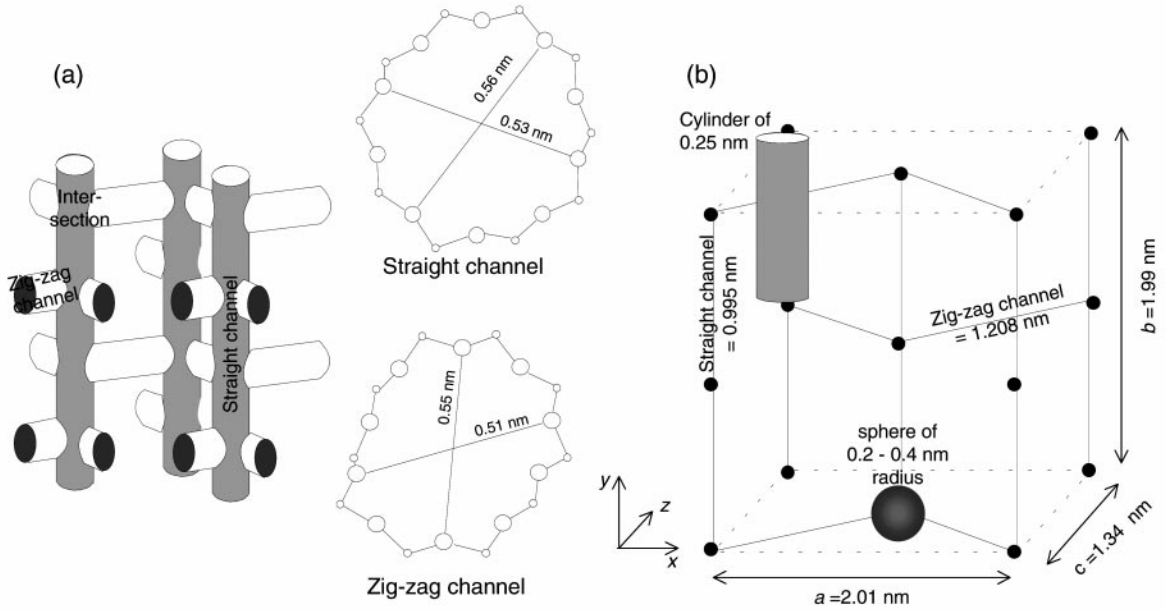

Fig. 1 (a) Schematic of structure of silicalite-1. (b) Diffusion unit cell for silicalite-1 connecting intersection sites (large black dots) *via* straight and zig-zag channels.

This journal is © The Owner Societies 2001

correlate both experimental data[14,17,18] and CBMC simulation results.[22,23,27] This 2SL model is necessary, in particular, to describe the inflection in the isotherm of branched alkanes.[17,18,22,23,27,30] In developing the 2SL model for the pure component isotherms, all authors have considered the two sites to be (A) channel intersections, and (B) channel interiors consisting of straight and zig-zag channels. Each of these "sites" has its distinct Langmuir constant (b_i) and saturation loading ($\Theta_{i,\,\mathrm{sat}}$). The 2SL model for the loading of component i at a pressure P, expressed in Pa, is

$$\Theta_i^0(P) = \frac{\Theta_{i,\,\mathrm{sat,\,A}}\, b_{i,\,\mathrm{A}}\, P}{1 + b_{i,\,\mathrm{A}}\, P} + \frac{\Theta_{i,\,\mathrm{sat,\,B}}\, b_{i,\,\mathrm{B}}\, P}{1 + b_{i,\,\mathrm{B}}\, P} \qquad (1)$$

The use of the 2SL model eqn. (1) implies that the straight and zig-zag channels have equal sorption strengths (b_i) and that molecules located at these two channel interior positions compete "en masse" with the molecules located at the channel intersections.

While there is a considerable amount of published experimental data on *pure* component sorption isotherms for various hydrocarbons,[12–18] there is little or no experimental data on *mixture* isotherms. This lack of mixture isotherm data is most probably due to the difficulty of experimentation. Kapteijn *et al.*[30] have recommended using the IAST for estimation of the sorption characteristics of mixtures using the 2SL model for the pure constituent isotherms with different saturation loadings.

Our first major objective in this paper is to investigate the validity of the assumptions underlying the 2SL model portrayed by eqn. (1) to describe pure component isotherms. In particular we wish to show that the lumping together of sites A and B to denote the channel intersections and channel interiors, respectively, is not justified. The approach we take is to use the CBMC technique to determine the equilibrium loadings separately for the straight and zig-zag channels and at the channel intersections.

The second objective is to investigate isotherms of various mixtures of light alkanes with a view to demonstrating that the mixture behaviour can be predicted from the pure component isotherms provided that the detailed molecular siting information is used.

2 CBMC simulation technique

Our simulations have been performed in the Grand Canonical ensemble wherein the zeolite is in contact with a reservoir that fixes the chemical potential of each component and also the temperature. In a CBMC simulation, it is essential to successfully exchange particles with the reservoir. With this technique we grow a flexible alkane molecule atom by atom in such a way that the "empty spaces" in the zeolite are found. The bias of this growing scheme is removed exactly by a modification of the acceptance rules.[27,34] The acceptance ratio of the particle exchange move is increased by 10 to 100 orders of magnitude and thus makes these simulations possible. To increase the efficiency of the mixture simulations, we also performed trial moves which change the identity of a particle. In the simulations presented in this work the linear and branched alkanes are described with a united-atom model, *i.e.* CH_3, CH_2 and CH groups are considered as single interaction centers. The bonded interactions include bond-bending and torsion potentials. The non-bonded interactions are described with a Lennard-Jones potential. The zeolite is modeled as a rigid crystal. The interactions of the alkane atoms with the zeolite atoms are dominated by dispersive interactions with the oxygen atoms; these interactions are described with a Lennard-Jones potential. The force-field parameters used in our simulations are the same as those reported in earlier work.[27]

Our simulation box consists of 16 ($2 \times 2 \times 4$) unit cells of silicalite. The simulations are performed in cycles; in each cycle an attempt is made to perform one of the following moves: (1) displacement of a chain: a chain is selected at random and given a random displacement; (2) rotation of a chain: a chain is selected at random and given a random rotation around the center of mass; (3) partial regrowing of a chain: a chain is selected at random and part of the molecule is regrown using the CBMC scheme; (4) exchange with reservoir using the CBMC scheme; it is decided at random whether to add or to remove a molecule from the zeolite; and (5) change of identity (only in the case of mixtures): one of the components is selected at random and an attempt is made to change its identity. The acceptance rules for this type of move are given elsewhere.[27,34] A total simulation consisted of at least 300 000 Monte Carlo cycles.

In order to be able to distinguish between different locations within the silicalite matrix, we have introduced a simple assignment-scheme based on the geometrical division of the adsorbed molecules accessible volume into different subvolumes. The position of every molecule is determined on the basis of its centre of mass position. First, the molecules belonging to an intersection site are obtained by drawing a sphere with a radius of 0.3 nm around each location of an intersection site; see Fig. 1(b). Since the intersection is not defined precisely in terms of a spherical region, we have also allowed the intersection region to be defined by a range of radii: 0.2, 0.25, 0.35 and 0.4 nm. The influence of the variation in the cut-off radius of the intersection region is discussed later. Next, the straight-channel site molecules are found within a cylinder oriented along the straight channel connecting two adjacent intersection sites and with a radius of 0.25 nm. Of course, only molecules which do not belong to the "intersection" subvolume, with its chosen cut-off radius are counted here. Finally, all other molecules are considered to belong to the zig-zag channel sites.

3 CBMC simulation results for pure components

Let us first consider the isotherm for isobutane at 300 K; the loading in the three different locations, determined from the CBMC simulations with a cut-off radius of 0.3 nm defining the intersection site, is shown in Fig. 2 as a function of pressure. The first thing to note is that the isobutane molecule prefers to locate at the intersections; this is evidenced by the fact that the Langmuir constant b_1 for the intersection site is 0.043 Pa^{-1}, more than three orders of magnitude higher than for the other locations. It is only for $P > 100$ kPa that the straight and zig-zag channels start to become occupied. A further point to note is that the Langmuir constant for the zig-zag channels ($b_1 = 1 \times 10^{-5}$ Pa^{-1}) is significantly higher than that of the straight channels ($b_1 = 1.2 \times 10^{-6}$ Pa^{-1}). At first sight, it therefore appears that there is no justification for combining the molecular loadings in the straight and zig-zag channels and considering these to be a single site, as has been done in the literature.[14,17,18,22,23,27,30] We also note from the simulation results in Fig. 2 that the Langmuir model provides a very good description of the loading at a given channel site. In view of the success of the Langmuir model there is no need to consider more advanced models taking molecular interactions into account, such as those presented by Ruthven.[3] The success of the Langmuir model as seen in Fig. 2 is to be traced to the fact that we apply this model *separately* to each of the three locations (straight channels, intersections and zig-zag channels). When the loadings of the locations are lumped together, interaction effects come into play as we shall see later.

Fig. 3 shows y-, and z-directional snapshots at 100 kPa, of the location of the isobutane molecules. The preponderance of isobutane molecules at the intersection sites is evident.

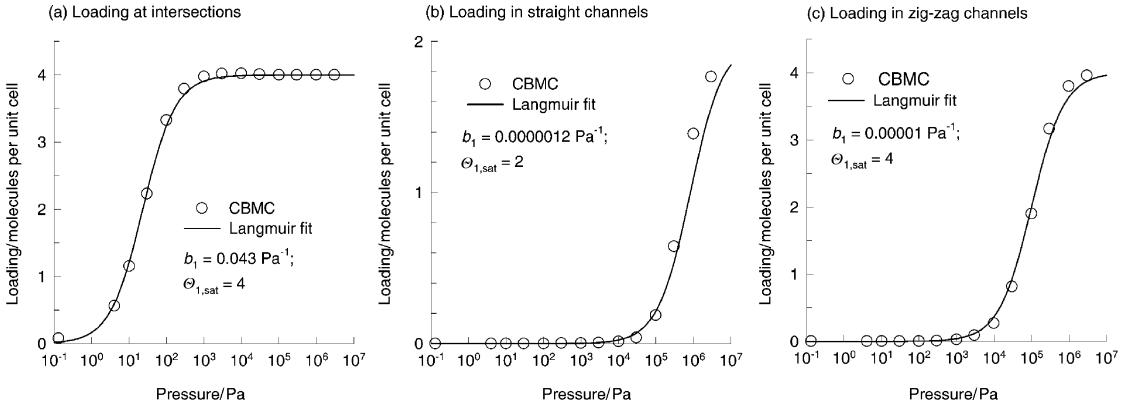

Fig. 2 Loadings of isobutane at 300 K in silicalite in (a) intersection sites, (b) straight channels and (c) zig-zag channels. The cut-off radius of sphere defining the intersection site is 0.3 nm.

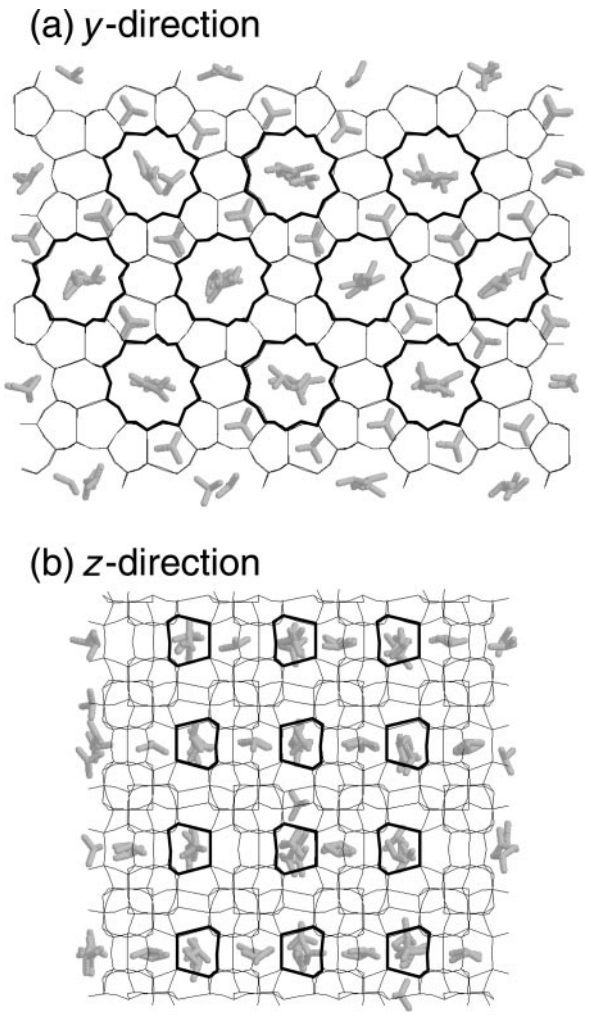

Fig. 3 Snapshot of the location of isobutane molecules at 100 kPa viewed in (a) *y*- and (b) *z*-directions as indicated in Fig. 1(b). The intersection region is indicated by heavy outline.

The siting of isobutane at different locations within the silicalite shown in Fig. 2 was obtained with a cut-off radius for the intersection sites of 0.3 nm. In view of the irregular geometry of the intersection region, we also considered other cut-off radii varying between 0.2 and 0.4 nm; the results are shown in Fig. 4. The choice of the cut-off radius does affect the distribution of molecules between the intersection and straight channels, while the loading in the zig-zag channels is scarcely affected. The straight and zig-zag channels are respectively 0.995 and 1.208 nm in length (distance between centers of the adjoining intersection sites). Since the straight channels are shorter, the loading here is more significantly influenced by the choice of the cut-off radius. If we sum the loading of the molecules in the straight channels and intersections (see Fig. 4(d)) we note that this sum is not significantly affected by the cut-off radius.

The loading in the zig-zag channels can be fitted with a single-site Langmuir model and the loading in the straight channels plus the intersections can be fitted with a 2SL model; the model parameters are listed in Table 1. The inflection behaviour of the isotherm for combined loading of the straight channels and intersections is clearly noticeable in Fig. 4(d) and underlines the need to plot the pressure using a logarithmic scale. The total loading is therefore described by a three-site Langmuir (3SL) model.

For n-butane the loadings in the three different locations are shown in Fig. 5. For this molecule the choice of the cut-off radius has a huge impact on the distribution between the straight channels and intersections. As for isobutane, the loading in the zig-zag channels is almost insensitive to the choice of the cut-off radius. Again, we consider it appropriate to sum the loadings of the straight channels and intersections (see Fig. 5(d)) and to fit this with a 2SL model; the model parameters are listed in Table 1.

To further appreciate why it is appropriate to sum the loadings in the straight channels and intersection sites, we present *y*- and *z*-directional snapshots of the siting of n-butane molecules at 100 kPa; see Fig. 6. Especially for the *z*-view we note that there is a continuous distribution of n-butane molecules

Table 1 Pure component Langmuir sorption parameters at 300 K in silicalite

	Zig-zag channels		Intersections + straight channels			
	$b_{i,\,A}$/Pa^{-1}	$\Theta_{i,\,sat}$	$b_{i,\,A}$/Pa^{-1}	$\Theta_{i,\,sat,\,A}$	$b_{i,\,B}$/Pa^{-1}	$\Theta_{i,\,sat,\,B}$
Isobutane	9.9×10^{-6}	4	0.043	4	1.8×10^{-6}	2
n-Butane	0.0174	4	0.0216	5	1.68×10^{-5}	1
Methane	2×10^{-6}	7	4×10^{-6}	7	2×10^{-7}	4
Ethane	6.42×10^{-5}	5	7.65×10^{-5}	6	7.39×10^{-5}	2
Propane	1×10^{-3}	4	9×10^{-4}	7	3×10^{-6}	1

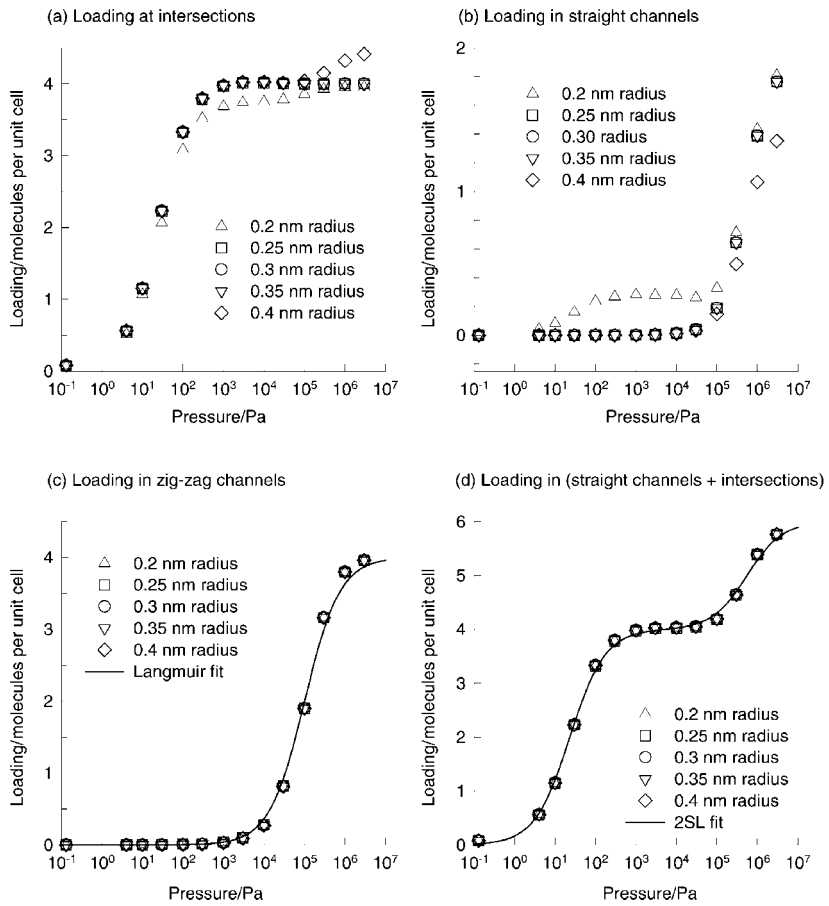

Fig. 4 Loadings of isobutane at 300 K in silicalite in (a) intersection sites, (b) straight channels, (c) zig-zag channels and (d) sum of straight channels and intersection sites. The cut-off radius of sphere defining the intersection site is varied as 0.2, 0.25, 0.3, 0.3 and 0.4 nm.

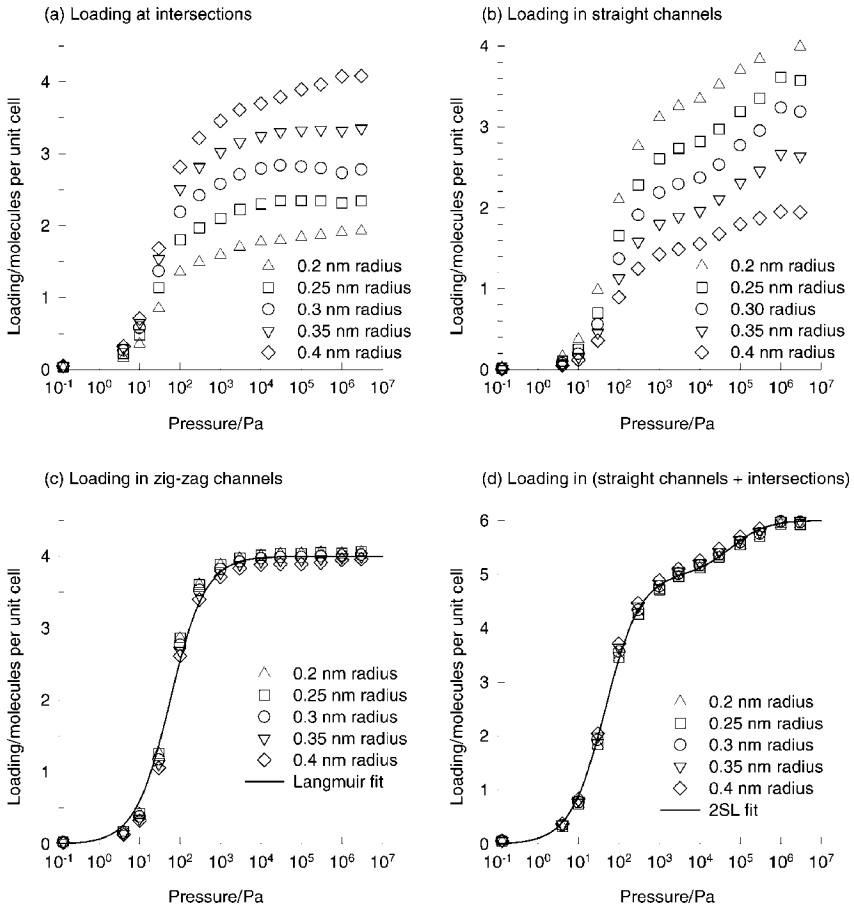

Fig. 5 Loadings of n-butane at 300 K in silicalite in (a) intersection sites, (b) straight channels, (c) zig-zag channels and (d) sum of straight channels and intersection sites. The cut-off radius of sphere defining the intersection site is varied as 0.2, 0.25, 0.3, 0.3 and 0.4 nm.

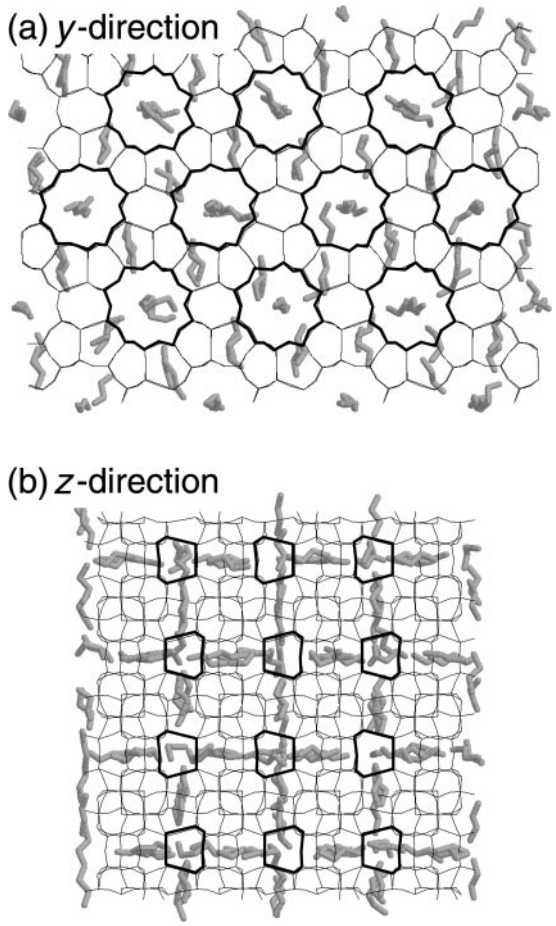

Fig. 6 Snapshot of the location of n-butane molecules at 100 kPa viewed in (a) *y*- and (b) *z*-directions as indicated in Fig. 1(b). The intersection region is indicated by heavy outline.

in the straight channels and intersections. Summing these two sites is therefore justified as these two locations "interact" with each other closely.

Situations analogous to that of n-butane hold for methane, ethane and propane; the loading information per site is given in Fig. 7–9. The model parameters are listed in Table 1.

From the 3SL parameters listed in Table 1, we can calculate the total loading for the pure components; these are compared in Fig. 10 with the experimental data of Sun *et al.*[16] and Zhu *et al.*[17,18] The agreement can be considered to be very good for methane, ethane and propane, good for n-butane and satisfactory for isobutane.

4 CBMC simulation results for mixtures compared with IAST predictions

CBMC simulations were also carried out for mixtures of methane–propane, methane–n-butane, n-butane–isobutane and propane–isobutane. These mixture simulations are compared with the predictions of the mixture loadings using the IAST of Myers and Prausnitz.[35] Briefly, the basic equation of IAST theory is the analogue of Raoult's law for vapour–liquid equilibrium, *i.e.*

$$Py_i = P_i^0(\pi)x_i \tag{2}$$

where x_i is the mole fraction in the adsorbed phase

$$x_i = \frac{\Theta_i}{\Theta_1 + \Theta_2} \tag{3}$$

and $P_i^0(\pi)$ is the pressure for sorption of every pure component i, which yields the same spreading pressure, π, as that for the mixture. The spreading pressure is defined by the Gibbs adsorption isotherm

$$\frac{\pi A}{k_B T} = \rho \int_{P=0}^{P=P_i^0} \frac{\Theta_i^0(P)}{P}\, dP \tag{4}$$

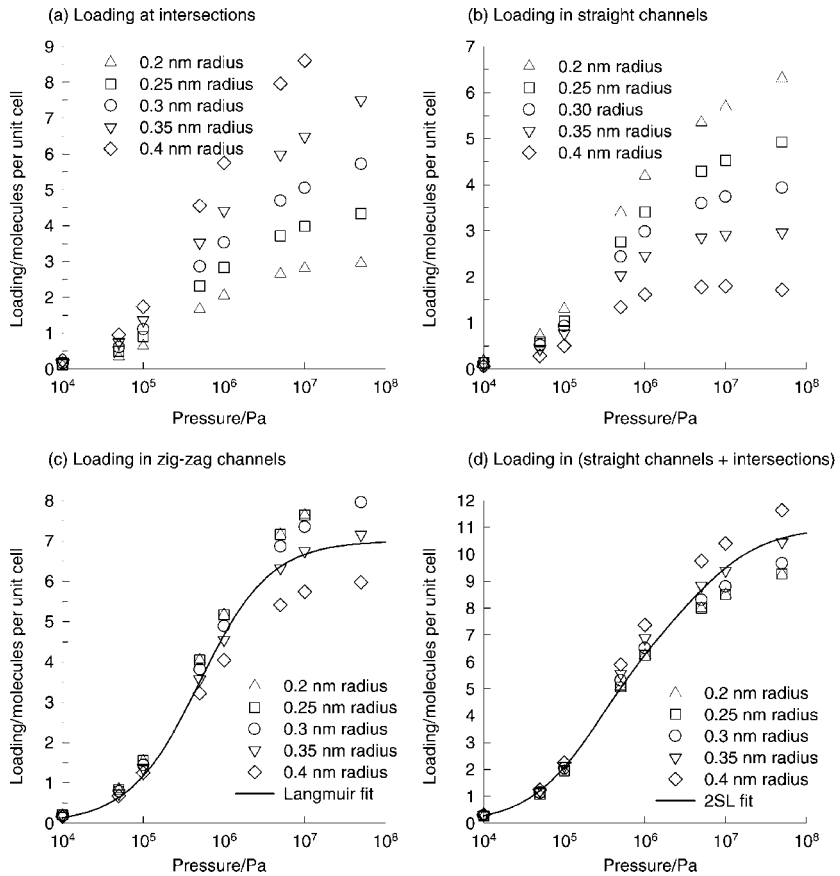

Fig. 7 Loadings of methane at 300 K in silicalite in (a) intersection sites, (b) straight channels, (c) zig-zag channels and (d) sum of straight channels and intersection sites. The cut-off radius of sphere defining the intersection site is varied as 0.2, 0.25, 0.3, 0.3 and 0.4 nm.

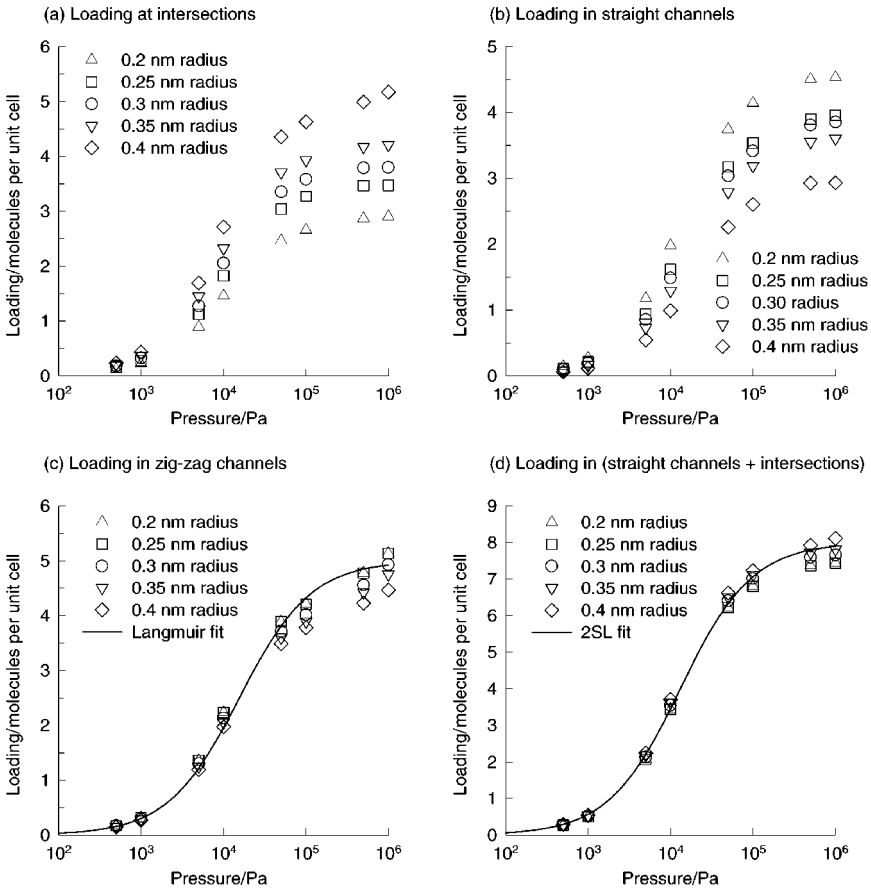

Fig. 8 Loadings of ethane at 300 K in silicalite in (a) intersection sites, (b) straight channels, (c) zig-zag channels and (d) sum of straight channels and intersection sites. The cut-off radius of sphere defining the intersection site is varied as 0.2, 0.25, 0.3, 0.3 and 0.4 nm.

where A is the surface area per m^3 of the adsorbent, k_B is the Boltzmann constant, ρ is the density of silicalite expressed in terms of the number of unit cells per m^3 and $\Theta_i^0(P)$ is the pure component isotherm given by eqn. (1). The IAS model implemented here calculates the absolute rather than excess sorption loadings. The total amount adsorbed is obtained from

$$\Theta_1 + \Theta_2 = \frac{1}{\dfrac{x_1}{\Theta_1^0(P_1^0)} + \dfrac{x_2}{\Theta_2^0(P_2^0)}} \quad (5)$$

The set of eqns. (1)–(5) need to be solved numerically to obtain the mixture loadings of components 1 and 2.

We first consider a 50 : 50 mixture of methane and propane at 300 K. The calculations of the IAST for mixture loadings in the (straight channels + intersections) and zig-zag channels *separately* using the pure component parameters listed in Table 1 are shown in Fig. 11(a) and (b) respectively. The mixture loadings are given in Fig. 11. The total mixture loading predicted using IAST compares very well with the CBMC simulations for the mixture; see Fig. 11(c). Fig. 12 shows the corresponding results for a 95 : 5 mixture of methane and n-butane at 300 K. Again we see that the total mixture loading predicted using IAST compares very well with the CBMC simulations for the mixture; see Fig. 12(c).

For both mixtures considered above, we note the increase in the methane loading at increased pressures. This is because of size entropy effects which tend to favour the smaller methane molecule at high loadings. The smaller methane molecule finds it much easier to fill in the "gaps" in the silicalite matrix as the loading increases. The IAST is able to capture the size entropy effects very well.

For a 50 : 50 mixture of n-butane and isobutane the loadings in the mixture are given in Fig. 13. In order to understand the mixture behaviour we present y- and z-directional snapshots of the siting of n-butane and isobutane molecules (at 100 kPa) in Fig. 14. We note from the snapshots that the isobutane molecules survive the mixture battle only at the intersection sites. These branched molecules are located nowhere else. Estimations of the mixture loadings using IAST also show that isobutane molecules shows that the branched molecules survive the battle at the intersections; see Fig. 13(a). The estimated mixture loading corresponds reasonably well with the CBMC mixture simulation results; see Fig. 13(c).

Let us now consider the 50 : 50 mixture of isobutane and propane at 300 K. This is an interesting mixture because the components differ in the number of C atoms. From this point of view isobutane should have a higher sorption strength than propane. However, isobutane exhibits an inflection behaviour. Therefore at increased pressures we should expect propane to be more selectively adsorbed. The predicted mixture loadings using IAST are shown in Fig. 15 where a clear selectivity reversal in the sorption behaviour is to be noted. The agreement with the CBMC mixture simulation results is fairly good.

5 Concluding remarks

The following major conclusions can be drawn:

1. CBMC simulations provide a powerful technique for determining the pure component and mixture isotherms of alkanes. The simulated pure component isotherms are in good agreement with experiment. There are no published experimental mixture isotherms and therefore CBMC simulations come into their own.

2. From the information on the detailed distribution of molecules in the straight and zig-zag channels and at the channel intersections, we conclude that in general we should adopt a 3SL model to describe the pure component isotherm. The

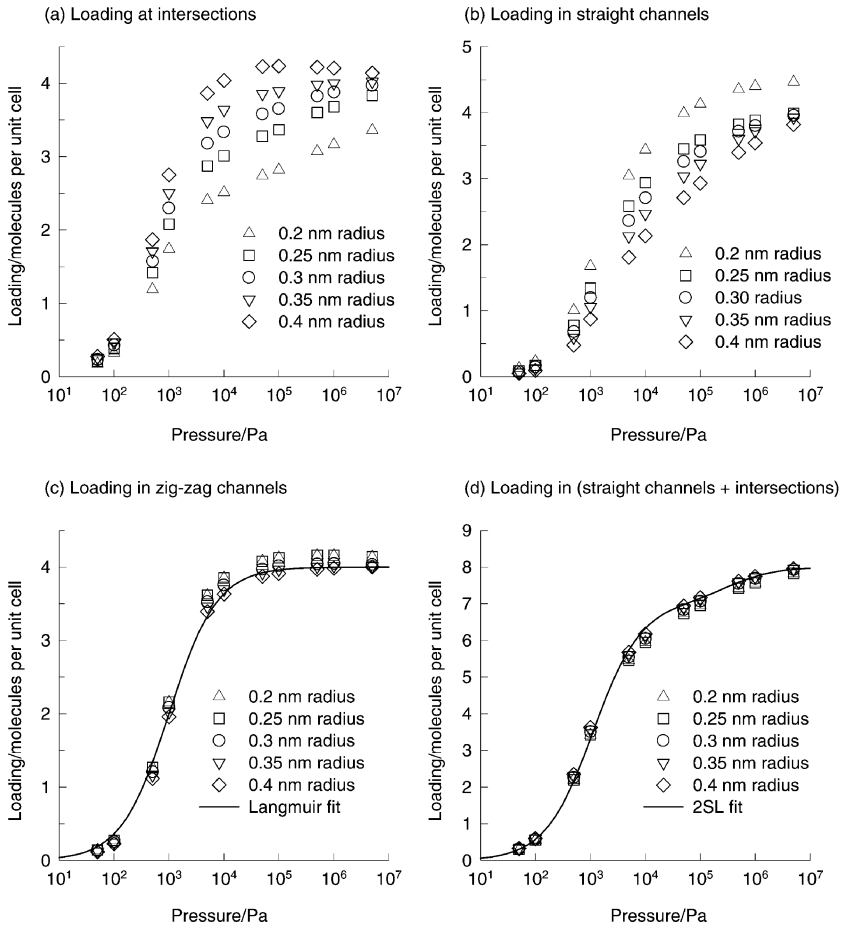

Fig. 9 Loadings of propane at 300 K in silicalite in (a) intersection sites, (b) straight channels, (c) zig-zag channels and (d) sum of straight channels and intersection sites. The cut-off radius of sphere defining the intersection site is varied as 0.2, 0.25, 0.3, 0.3 and 0.4 nm.

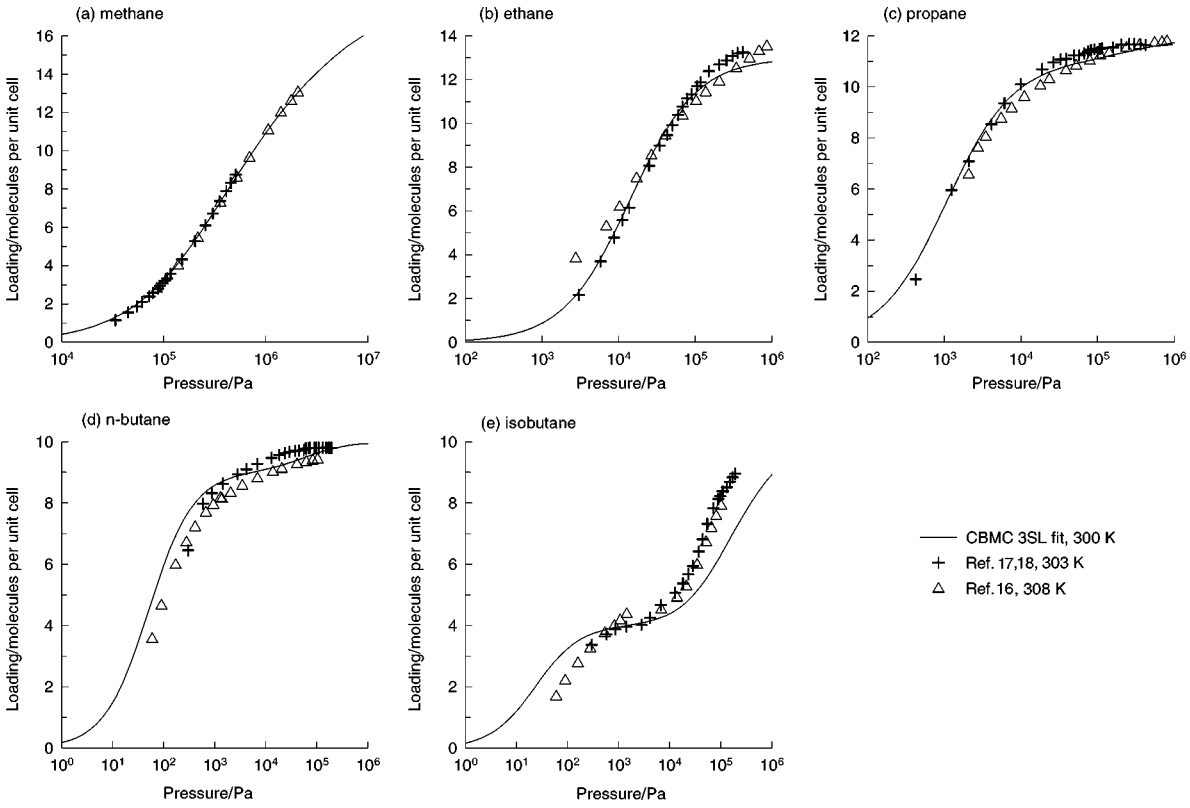

Fig. 10 Comparison of the experimental data for pure component isotherms for (a) methane, (b) ethane, (c) propane, (d) n-butane and (e) isobutane with 3SL fits of CBMC simulations using the parameters given in Table 1.

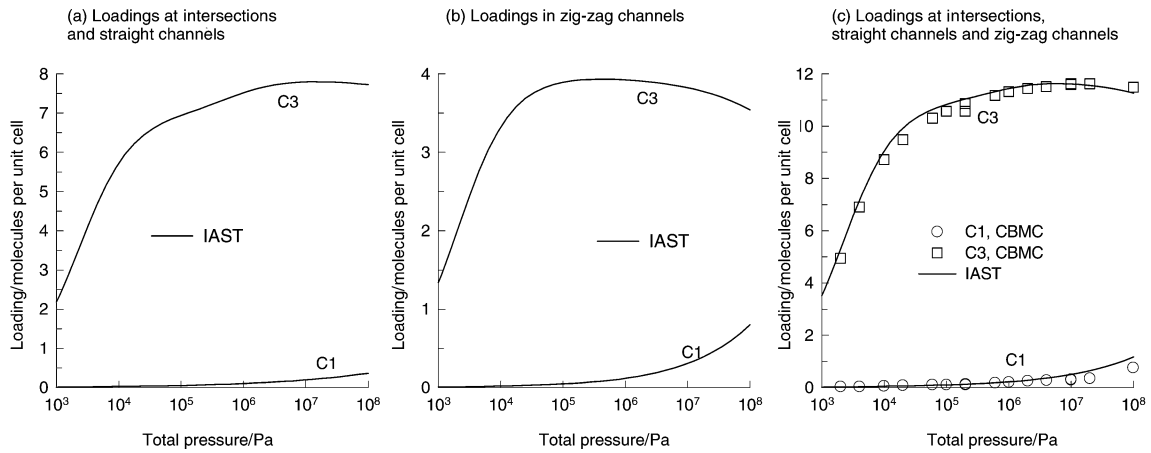

Fig. 11 Loading of 50 : 50 mixture of methane and propane in silicalite. (a) Predictions of IAST for mixture loading in the (straight channels + intersections). (a) Predictions of IAST for mixture loading in the zig-zag channels. (c) Comparison of IAST predictions for total loading within silicalite with CBMC mixture simulations.

fitted 3SL model shows good agreement with the experimental data on pure component sorption of light alkanes.

3. In the literature the 2SL model is used to describe the pure component isotherm, wherein the characteristics of the straight and zig-zag channels are lumped together. We have obtained detailed information on the loadings at these three separate locations and have concluded that there is no real justification for summing the molecules in the straight and zig-zag channels. Furthermore, because the straight channels are significantly shorter than the zig-zag channels, there

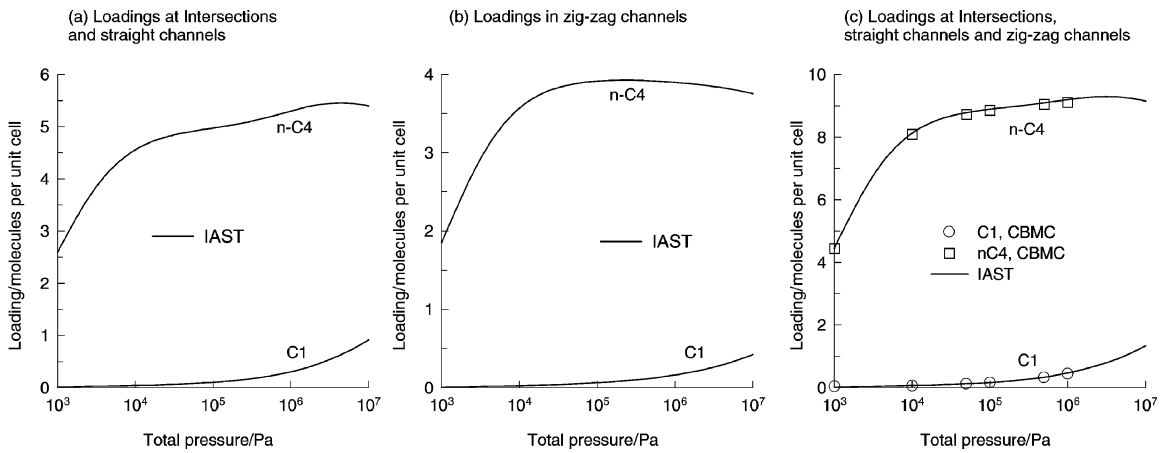

Fig. 12 Loading of 95 : 5 mixture of methane and n-butane in silicalite. (a) Predictions of IAST for mixture loading in the (straight channels + intersections). (a) Predictions of IAST for mixture loading in the zig-zag channels. (c) Comparison of IAST predictions for total loading within silicalite with CBMC mixture simulations.

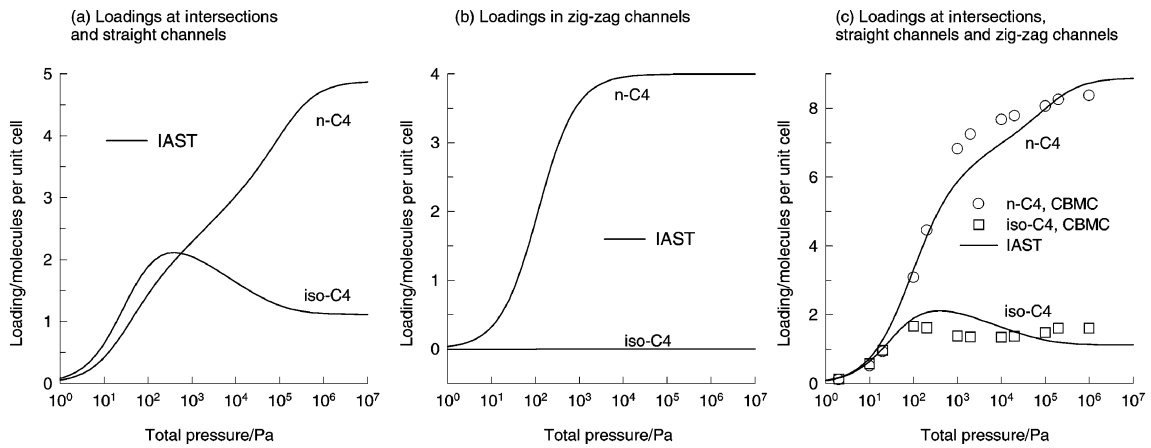

Fig. 13 Loading of 50 : 50 mixture of n-butane and isobutane in silicalite. (a) Predictions of IAST for mixture loading in the (straight channels + intersections). (a) Predictions of IAST for mixture loading in the zig-zag channels. (c) Comparison of IAST predictions for total loading within silicalite with CBMC mixture simulations.

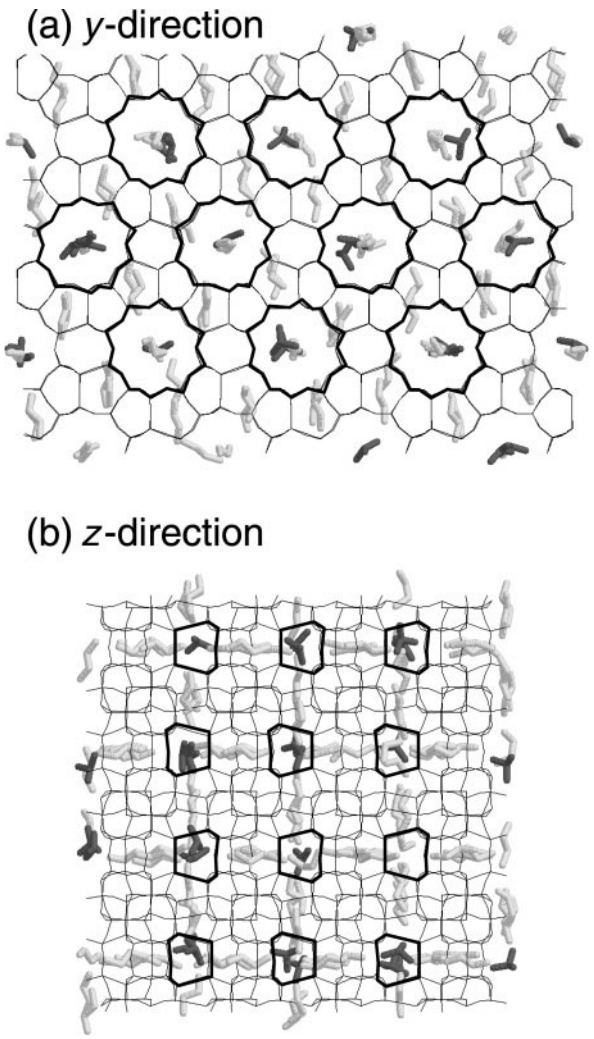

Fig. 14 Snapshot of the location of 50 : 50 mixture of n-butane and isobutane molecules at 100 kPa viewed in (a) *y*- and (b) *z*-directions. The intersection region is indicated by heavy outline.

appears to be an almost continuous distribution of molecules in the straight channels and intersections. For this reason we consider it more logical to sum the loadings of the straight channels and the intersection sites. The combined loading is very well described by a 2SL model; the parameters for light alkanes at 300 K have been presented in Table 1.

4. By applying IAST to the zig-zag channels and (straight channels + intersections) separately, the predicted mixture behaviour is in good agreement with CBMC mixture simulations.

6 Acknowledgements

The authors acknowledge a grant *Programmasubsidie* from the Netherlands Organisation for Scientific Research (NWO) for

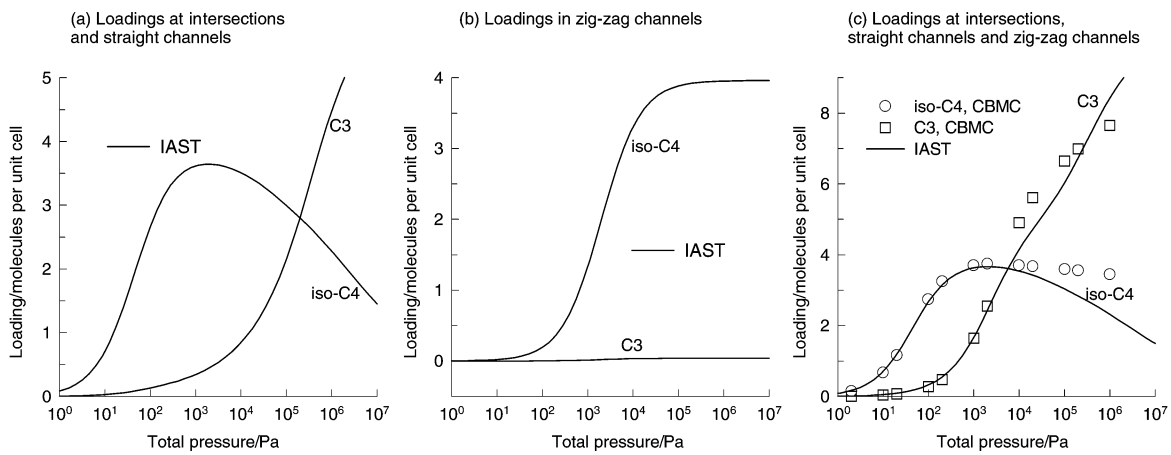

Fig. 15 Loading of 50 : 50 mixture of isobutane and propane in silicalite. (a) Predictions of IAST for mixture loading in the (straight channels + intersections). (a) Predictions of IAST for mixture loading in the zig-zag channels. (c) Comparison of IAST predictions for total loading within silicalite with CBMC mixture simulations.

development of novel concepts in reactive separations technology. The CBMC simulations were carried out using the program, written by T. J. H. Vlugt. J. M. van Baten provided valuable programming assistance.

References

1 K. Huddersman and M. Klimczyk, *A.I.Ch.E.J.*, 1996, **42**, 405.
2 J. Kärger and D. M. Ruthven, *Diffusion in Zeolites and Other Microporous Solids*, Wiley, New York, 1992.
3 D. M. Ruthven, *Principles of Adsorption and Adsorption Processes*, Wiley, New York, 1984.
4 H. H. Funke, A. M. Argo, J. L. Falconer and R. M. Noble, *Ind. Eng. Chem. Res.*, 1997, **36**, 137.
5 J. Van de Graaf, F. Kapteijn and J. A. Moulijn, *A.I.Ch.E.J.*, 1999, **45**, 497.
6 C. J. Gump, R. D. Noble and J. L. Falconer, *Ind. Eng. Chem. Res.*, 1999, **38**, 2775.
7 H. H. Funke, K. R. Frender, K. M. Green, J. L. Wilwerding, B. A. Sweitzer, J. L. Falconer and R. M. Noble, *J. Membr. Sci.*, 1997, **129**, 77.
8 A. Tavolaro and E. Drioli, *Adv. Mater.*, 1999, **11**, 975.
9 X. Lin, J. L. Falconer and R. M. Noble, *Chem. Mater.*, 1998, **10**, 3716.
10 P. Ciaverella, H. Moueddeb, S. Miachon, K. Fiaty and J. A. Dalmon, *Catal. Today*, 2000, **56**, 253.
11 T. Matsufuji, K. Watanabe, N. Nishiyama, Y. Egashira, M. Matsukata and K. Ueyama, *Ind. Eng. Chem. Res.*, 2000, **39**, 2434.
12 L. Boulicaut, S. Brandani and D. M. Ruthven, *Microporous Mesoporous Mater.*, 1998, **25**, 81.
13 C. L. Cavalcante, Jr. and D. M. Ruthven, *Ind. Eng. Chem. Res.*, 1995, **35**, 177.
14 B. Millot, A. Methivier and H. Jobic, *J. Phys. Chem. B*, 1998, **102**, 3210.
15 M. S. Sun, O. Talu and D. B. Shah, *J. Phys. Chem.*, 1996, **100**, 17276.
16 M. S. Sun, D. B. Shah, H. H. Xu and O. Talu, *J. Phys. Chem.*, 1998, **102**, 1466.
17 W. Zhu, F. Kapteijn and J. A. Moulijn, *Phys. Chem. Chem. Phys.*, 2000, **2**, 1989.
18 W. Zhu, F. Kapteijn and J. A. Moulijn, *Adsorption*, 2000, **6**, 159.
19 J. M. van de Graaf, F. Kapteijn and J. A. Moulijn, *Microporous Mesoporous Mater.*, 2000, **35**, 267.
20 M. D. Macedonia and E. J. Maginn, *Fluid Phase Equilib.*, 1999, **150**, 19.
21 Z. Du, G. Manos, T. J. H. Vlugt and B. Smit, *A.I.Ch.E. J.*, 1998, **44**, 1756.
22 R. Krishna, B. Smit and T. J. H. Vlugt, *J. Phys. Chem. A*, 1998, **102**, 7727.
23 R. Krishna, T. J. H. Vlugt and B. Smit, *Chem. Eng. Sci.*, 1999, **54**, 1751.
24 R. Krishna and D. Paschek, *Ind. Eng. Chem. Res.*, 2000, **39**, 2618.
25 R. Krishna and L. J. P. van den Broeke, *Chem. Eng. J*, 1995, **57**, 155.
26 T. J. H. Vlugt, W. Zhu, F. Kapteijn, J. A. Moulijn, B. Smit and R. Krishna, *J. Am. Chem. Soc.*, 1998, **120**, 5599.
27 T. J. H. Vlugt, R. Krishna and B. Smit, *J. Phys. Chem. B*, 1999, **103**, 1102.
28 R. Krishna and J. A. Wesselingh, *Chem. Eng. Sci.*, 1997, **52**, 861.
29 D. Paschek and R. Krishna, *Chem. Phys. Lett.*, 2001, **333**, 278.
30 F. Kapteijn, J. A. Moulijn and R. Krishna, *Chem. Eng. Sci.*, 2000, **55**, 2923.
31 D. Paschek and R. Krishna, *Phys. Chem. Chem. Phys.*, 2000, **2**, 2389.
32 R. Krishna, *Chem. Phys. Lett.*, 2000, **326**, 477.
33 R. Krishna and D. Paschek, *Sep. Purif. Technol.*, 2000, **21**, 111.
34 T. J. H. Vlugt, M. G. Martin, J. I. Siepmann, B. Smit and R. Krishna, *Mol. Phys.*, 1998, **94**, 727.
35 A. L. Myers and J. M. Prausnitz, *A.I.Ch.E. J.*, 1965, **11**, 121.